Manuscript Details

Manuscript number	POC_2019_796_R1
Title	A contrastive investigation on anticorrosive performance of laser-induced super-hydrophobic and oil-infused slippery coatings
Article type	Research Paper

Abstract

Nature inspired super-hydrophobic surface has aroused extensive attention on corrosion prevention. More works have investigated the instant corrosion resistance of fresh super-hydrophobic surface, but less research focused on its stability when immersed into corrosive solution for long time. Recently, another bio-mimic surface with slippery coating also presented great corrosion inhibition due to its excellent insulation between the corrosive medium and base material. However, which coating is suitable for long-term immersion into corrosive environments still remains to investigate. Herein, we firstly fabricated a super-hydrophobic coating on 316L stainless steel by nanosecond laser ablation combining fluoroalkylsilane modification. Then a slippery coating was obtained by further infusing silicon oil into the as-prepared super-hydrophobic substrate. The PDP and EIS measurements indicate that both fresh super-hydrophobic and slippery surface were observed to improve the corrosion inhibition for the base substrate, and the performance of slippery surface was superior to that of super-hydrophobic surface. Immersion experiments infer that the air cushion of the super-hydrophobic surface was easily destroyed, resulting in a rapid failure of super-hydrophobicity and instability of corrosion resistance. In contrast, after immersed into 3.5 wt.% NaCl solution, the wetting property of oil-impregnated slippery surface almost remained the same. In addition, the electrochemical measurements reveal that the slippery coating presented exceptional anticorrosion behavior after long-term immersion into corrosive liquid. Therefore, the authors believe this study is expected to promote the development of anticorrosive coating for the steel materials. This work is of great importance for employing laser ablation to fabricate slippery surface, which is convenient and effective for metallic corrosion prevention in industrial fields.

Keywords	Laser ablation; Super-hydrophobic; Oil-infused slippery; Corrosion prevention; Stability

Corresponding Author	Yanling Tian
Corresponding Author's Institution	Tianjin University
Order of Authors	Zhen Yang, Xianping Liu, Yanling Tian
Suggested reviewers	Takahiro Ishizaki, Kyle Jiang, Guangneng Dong, Yan Liu, Wenjun Wang

Submission Files Included in this PDF

File Name [File Type]

Cover letter.docx [Cover Letter]

Response to Reviewers.docx [Response to Reviewers]

Highlights.docx [Highlights]

Graphical Abstract.docx [Graphical Abstract]

Revised Manusript.docx [Manuscript File]

Supporting Information.docx [e-Component]

Submission Files Not Included in this PDF

File Name [File Type]

Movie S1.mp4 [Video]

Movie S2.mp4 [Video]

To view all the submission files, including those not included in the PDF, click on the manuscript title on your EVISE Homepage, then click 'Download zip file'.

Progress in Organic Coatings

13 August 2019

Dear Editor,

On behalf of all authors, I would like to say many thanks to you for giving us the opportunity to revise our manuscript. We highly appreciate you and the reviewers for the positive and constructive remarks dedicated to our paper entitled "**A contrastive investigation on anticorrosive performance of laser-induced super-hydrophobic and oil-infused slippery coatings**".

In order to cooperate the reviewers' comments, the Introduction Section has been significantly improved based on the reviewer's suggestions. Then, two reference samples (laser-processing surface and pristine surface with silicon oil) have been also investigated in terms of the wetting property and anticorrosive performance. In addition, the surface chemical components of the super-hydrophobic surfaces were detected after they were immersed into NaCl solution for 0h, 12h, 24h, 48h, and 72h. The results indicate that the fluorine content experienced a continuous decrease with the increase of immersion time. The failure mechanism of super-hydrophobicity as well as corrosion resistance was detailly discussed based on the modifications of surface structure and surface chemical components. Finally, the figures, tables and languages of the whole text have been carefully checked and modified to satisfy the requirements of ***Progress in Organic Coatings***.

Attached please find our revised format of manuscript, which we would like to submit for your further consideration. Thanks very much.

Yours sincerely,

Yanling Tian

School of Engineering

University of Warwick, Coventry CV4 7AL, UK

Email: meytian@tju.edu.cn , Y.Tian.1@warwick.ac.uk

Detailed Response to Comments

Reviewer 1:

This paper proposes a new anti-corrosion process, which involves laser ablation to create a microstructure surface and fluoroalkylsilane treatment of the surface before a silicon coating is applied. Extensive experiments were conducted for characterisation of the surface. The process is unique and has engineering value. The anti-corrosion surface can last longer than other typical coatings. It is recommended that the paper should be improved in its presentation before it can be published.

[Authors' Response]: The authors would like to thank the reviewer's time and efforts on our manuscript. We are delighted that the reviewer confirmed the engineering value of our research. The manuscript has been carefully checked and revised point by point according to the reviewer's comments.

1. For example, the first sentence of the paper states "Corrosion is costly, more than US$ 4 trillion annually in the world [1]" is not correct in structure and should be changed to "Corrosion costs more than US$ 4 trillion annually in the world [1]."

[Authors' Response]: Thanks for your comment. Based on the above advice, the first sentence of this manuscript has been revised. (See Line 33 on Page 2).

2. In the first sentence of the second paragraph of the paper, the word "literatures" should be changed to "literature".

[Authors' Response]: We appreciate the reviewer's attention to detail, and we have corrected the word "literatures" to "literature" as suggested. (See Line 54 on Page 2).

3. The list goes on. The authors should smooth up the presentation of the paper before

submitting it again.

[Authors' Response]: Thanks for this comment. The whole text in this manuscript has been carefully checked and modified to avoid any grammatical mistake. The presentation of this paper has been polished to make it easily understood. (See the changes highlighted by yellow color in the revised manuscript).

Reviewer 2:

1. This paper reports on the comparison of anticorrosive performance of the super-hydrophobic surface and oil-infused slippery surface. The surface micro/nano structure was produced with nanosecond laser, the super-hydrophobic property is obtained with fluoroalkylsilane modification, and the slippery surface is obtained with lubricating silicon oil. The result in the paper shows the oil-infused slippery surface has better anticorrosive performance. This work has certain contribution to the engineering application.

[Authors' Response]: The authors highly appreciate your time and efforts to review our manuscript. We are delighted to receive reviewer's positive evaluation of our work as well as insightful comments. We have tried our best to incorporate the reviewer's suggestions and comments, and the detailed responses are provided as below.

Introduction:

1. Author says that "stainless steel has a wide range of applications in many areas, including water pipelines, storage tank, heat exchanger, handrail, building construction, and so forth". While, the addition of fluoroalkylsilane modification and the lubricating

silicon oil would affect the usage of the stainless steel. In this way, the application of the stainless steel would be limited. In addition, conventional method to prevent the stainless steel from corrosion also should be introduced, such as coating technology.

[Authors' Response]: Thanks very much for these insightful comments. The authors strongly agree with the reviewer that the usage of stainless steel will be influenced by the modifications of fluoroalkylsilane and lubricating silicon oil. Therefore, in the revised manuscript, the applications of stainless steel with super-hydrophobic and slippery surface have been modified. It can be expected that based on the addition of fluoroalkylsilane modification and silicon oil coating, stainless steel can be more suitably utilized in sewage pipeline, marine vessel, underground and submarine cables, etc. (See Lines 36-38 on Page 2; Lines 124-127 on Page 5).

Furthermore, according to the reviewer's advice, the conventional method to prevent stainless steel from corrosion has been introduced in Introduction Section, which is the usage of protective coatings, including organic coating, polymeric coating, graphite coating, Ni-P coating, and ceramic coating. Although these protective coatings can improve corrosive resistance of steel substrate to some extent, they have some drawbacks due to poor adhesion and the presence of pores or cracks during the fabrication process. Therefore, more alternative strategies should be exploited to further improve the anticorrosive performance of steel for long-term stability. The first paragraph of Introduction has been modified in order to satisfy the reviewer's comment. The relevant papers have been cited and added in the Reference list accordingly. (See Lines 36-53 on Page 2).

2. In this paper, the super-hydrophobic surface is obtained via nanosecond laser irradiation and fluoroalkylsilane modification. Author should introduce the method to produce the super-hydrophobic surface, and the reason for choose of laser processing. In general, this two kinds of laser processing to produce super-hydrophobic surface. The first method is purely based on micro/nano structure, see "Pan A, Wang W, Mei X, et al. Rutile TiO_2 Flocculent Ripples with High Antireflectivity and Superhydrophobicity on the Surface of Titanium under 10 ns Laser Irradiation without Focusing [J]. Langmuir, 2017, 33(38): 9530-9538." Other method is based on laser processing and fluoroalkylsilane modification. See "Zheng B, Jiang G, Wang W, et al. Fabrication of superhydrophilic or superhydrophobic self-cleaning metal surfaces using picosecond laser pulses and chemical fluorination [J]. Radiation Effects and Defects in Solids, 2016, 171(5-6): 461-473."

[Authors' Response]: Thanks for your comments and recommended papers. The conventional methods to produce super-hydrophobic surfaces have been introduced, such as thermal embossing, chemical etching, chemical vapor deposition, sol-gel, electrodeposition, and hydrothermal reaction, etc. Due to tedious chemical preparation, multiple processing steps and expensive equipment, the above-mentioned methods will limit the fabrication efficiency. (See Lines 56-62 on Pages 2-3). On the contrary, laser processing is recently regarded as a convenient and green approach to produce super-hydrophobic surfaces because it can create micro/nano structures with high processing accuracy and low thermal damage. In addition, through precise control of laser parameters, stable three dimensional (3D) hierarchical surface texture can be obtained

without polluting environment. Therefore, we used laser processing to fabricate super-hydrophobic and slippery surfaces in this current paper. (See Lines 62-67 on Page 3). Besides, as suggested by reviewer, two kinds of laser processing methods to produce super-hydrophobic surfaces have been added in the Introduction Section. The recommended papers have been added to Refs. 21-22. (See Lines 67-70 on Page 3).

[21] B.X. Zheng, G.D. Jiang, W.J. Wang, X.S. Mei, Fabrication of superhydrophilic or superhydrophobic self-cleaning metal surfaces using picosecond laser pulses and chemical fluorination, Radiat. Eff. Defects Solids 171 (2016) 461-473.

[22] A.F. Pan, W.J. Wang, X.S. Mei, K.D. Wang, X.B. Yang, Rutile TiO_2 flocculent ripples with high antireflectivity and superhydrophobicity on the surface of titanium under 10 ns laser irradiation without focusing, Langmuir 33 (2017) 9530-9538.

Result:

1. The pristine surface, laser-processing surface, super-hydrophobic surface, the pure slippery surface with silicon oil, and the super-hydrophobic surface with silicon oil, should be compared in the term of hydrophobicity and anticorrosive performance. It is known that the saline water can clean the fluoride on the surface. Therefore, it should be depicted the fluoride content change with the time, as the hydrophobicity changes with the time. In addition, the anticorrosive performance change mechanism is should be discussed in detail. Then, the role of the surface structure, the chemical content on the anticorrosive performance should be discussed.

[Authors' Response]: We thank the reviewer for these valuable comments. In our original format of manuscript, the hydrophobicity and anticorrosive performance of the

pristine 316L stainless steel, as-prepared super-hydrophobic and slippery samples had been investigated. In this revised format of manuscript, in order to satisfy the reviewer's concerns, the laser-processing surface and pure slippery surface with silicon oil (i.e., pristine 316L substrate with silicon oil coating) were further explored and compared in terms of hydrophobicity and corrosion resistance. (See Lines 164-166 on Page 6; Lines 281-284 on Page 11).

In terms of the hydrophobicity, the WCA values of the laser-processing surface and the pristine surface with silicon oil have been measured and depicted in Fig. S1, as shown in the Supporting Information. The reasons of WCA changes were also explained, which was added in Section 3.2. of the revised manuscript. (See Lines 268-275 on Page 11; Fig. S1 in Supporting Information).

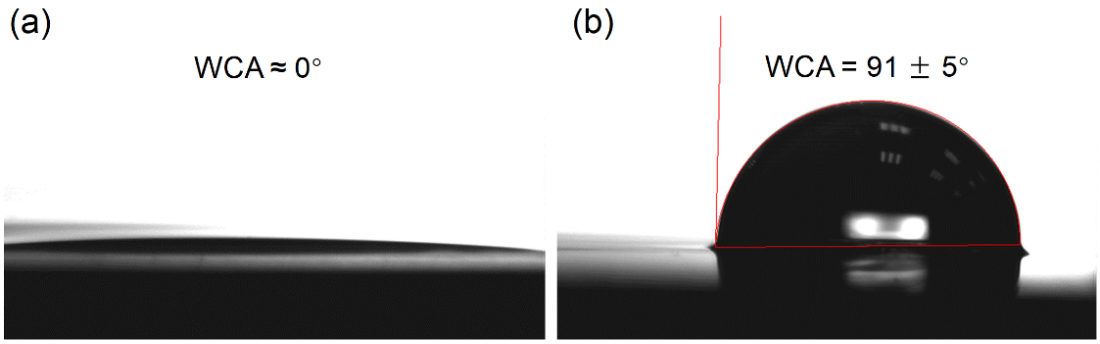

Figure S1. WCA values of (a) initial laser-processing surface, (b) pristine 316L substrate with silicon oil coating.

In terms of the anticorrosive performance, the PDP curves of the laser-processing surface and pristine surface with silicon oil were measured in the 3.5 wt.% NaCl solution. Fig. 4 and Table 1 have been modified accordingly. In addition, the EIS plots of the laser-processing surface and the pristine surface with silicon oil were also examined, and the results have been added in Fig. S2 and Table S1. The corresponding analyses and comparisons have been added in Section 3.3.1. of the revised manuscript.

(See Lines 309-324, 330-336 on Page 13; Lines 351-360 on Page 14; Lines 381-382 on Page 15; Fig. 4 and Table 1 on Page 12; Fig. S2 and Table S1 in Supporting Information).

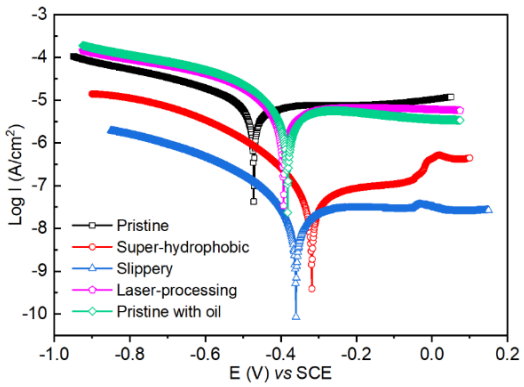

Figure 4. PDP curves for the studied samples.

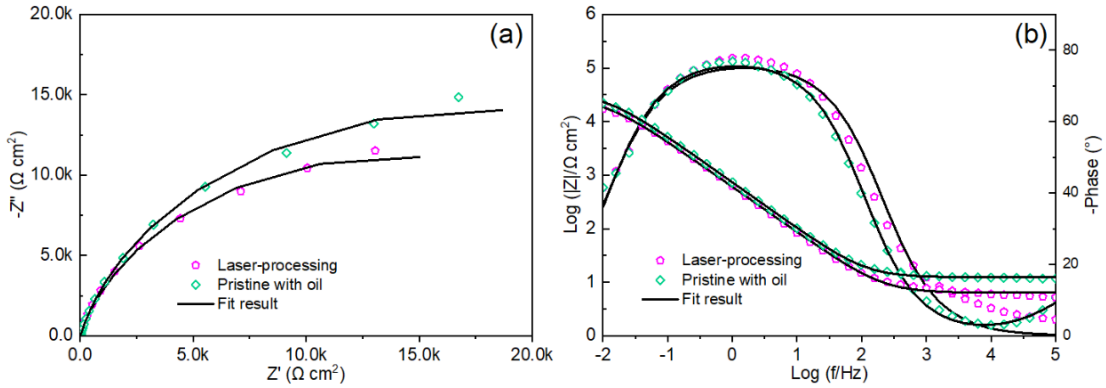

Figure S2. (a) Nyquist plots and (b) Bode Plots of the initial laser-processing surface and pristine 316L substrate with silicon oil coating. The fit result was received based on the equivalent circuit displayed in Fig. 5b.

In terms of the fluoride content on the as-prepared super-hydrophobic surface, the authors strongly agree with the reviewer that saline water can clean the fluoride component during the immersion period, resulting in the modification of hydrophobicity. Therefore, it is better to detect the changes of fluoride content under different immersion time into corrosive solution. In the revised manuscript, the fluoride contents of the super-hydrophobic samples under 0, 12, 24, 48, 72 hours immersion time were detected by energy-dispersive spectroscopy (EDS), and the results were

displayed in Fig. 7. The analyses and comparisons have been added in Section 3.3.2. of the revised manuscript. (See Lines 421-428 on Page 17; Fig. 7 on Page 18).

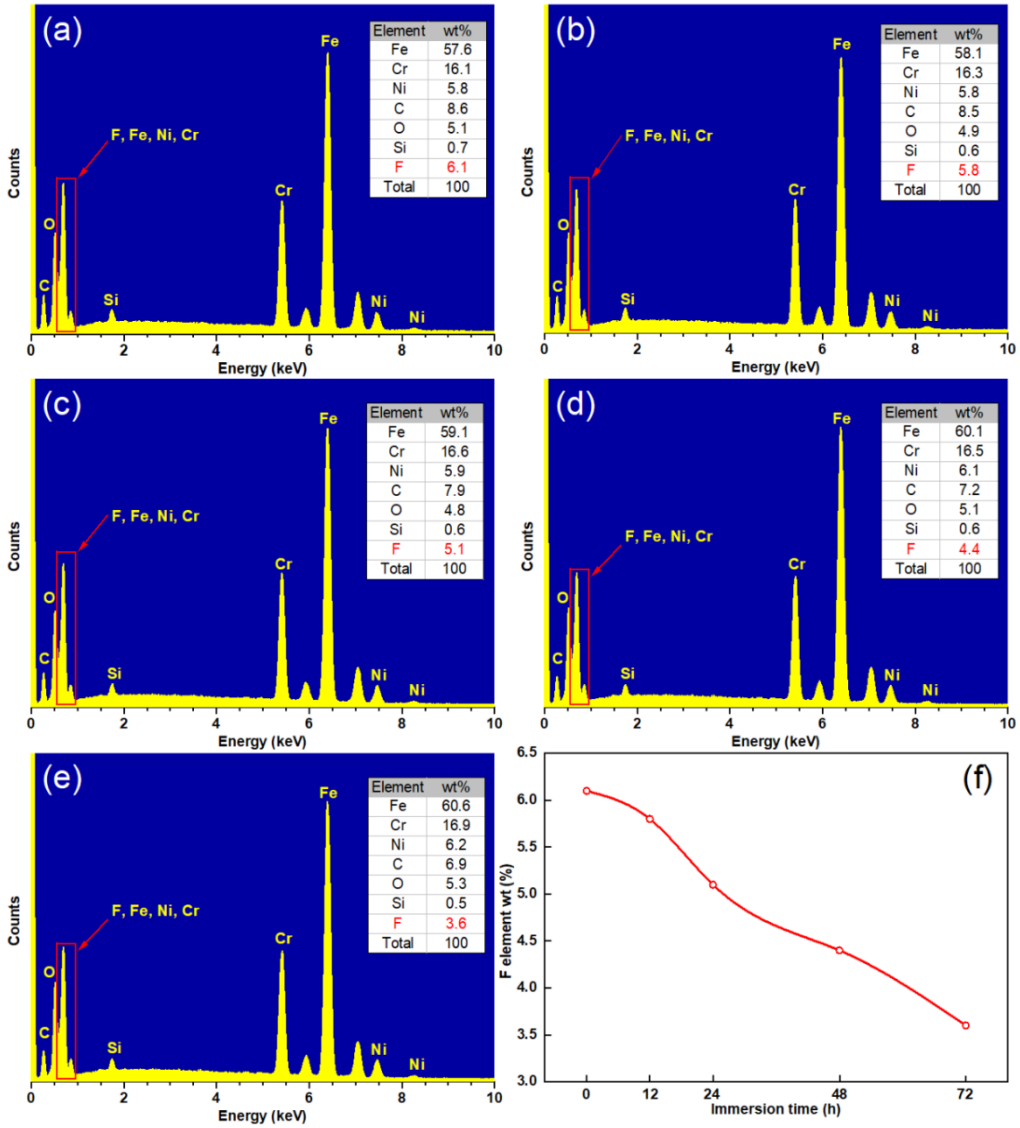

Figure 7. EDS spectra of the as-prepared super-hydrophobic surfaces after immersion into NaCl solution for (a) 0 h, (b) 12 h, (c) 24 h, (d) 48 h, (e) 72 h; (f) the changes of fluorine content with immersion time.

In terms of the change mechanism of corrosion resistance performance, both the surface structures and surface chemical components play important role in anticorrosive performance when the as-prepared super-hydrophobic surfaces were immersed into corrosive solution. Based on the generation of surface cracks and decrease of fluorine

content, the change mechanism of anticorrosive performance has been analyzed and discussed in detail. (See Lines 421-438 on Page 17).

2. As shown in the figure 1, are the SEM images before cleaning or after cleaning? In general, for nanosecond laser processing, the surface deposition as shown in inset "c" may be removed after cleaning. In this regard, the deposition would not take a role in the anticorrosive performance.

[Authors' Response]: Thanks for your question. Some of fabrication procedures were ambiguous, and we have modified the text to be more clear. (See Lines 151-154 on Page 6). In fact, after laser ablation process, the processed sample was firstly flushed by distilled water and then blown by the compressed nitrogen gas. Therefore, the SEM images in Fig. 1 were obtained after cleaning.

The authors indeed saw some debris and ash residues were produced during the laser treatment. We agree with the reviewer that these kinds of surface deposition cannot make a difference in the surface wettability and anticorrosive performance. Therefore, the laser-ablated samples should be cleaned before fluoroalkyl-silane modification. However, Fig. 1c is a magnified SEM image of the laser-induced particles. The formation mechanism has been analyzed in the first paragraph in Section 3.1. (See Lines 198-203 on Page 8). Due to the laser ablation, the interfacial materials will be removed and ejected in the form of molten particles with micro/nano-scaled size. Then some molten particles will fall back and re-solidified onto the sample surface with a high adhesive force. The similar surface morphology of nanosecond laser-induced 316L stainless steel can be observed in previous literature [1]. Long et al. proved that even

after ultrasonically cleaned by ethanol and then dried by compressed air, the produced particles on the laser-induced samples cannot be removed [2].

Thanks for this valuable comment, and the authors have stressed that the entrapped air among the laser-induced rough structures with pits array play an important role in anticorrosive performance for the as-prepared super-hydrophobic surface. Besides, for the as-prepared slippery surface, the best anticorrosion performance is due to the laser-induced pits array anchoring the insulating silicon oil coating. (See Section 3.3.).

[1] P. Gregorčič, B. Šetina□Batič, M. Hočevar, Controlling the stainless steel surface wettability by nanosecond direct laser texturing at high fluences, Appl. Phys. A (2017) 123-766.

[2] J. Long, M. Zhong, H. Zhang, P. Fan, Superhydrophilicity to superhydrophobicity transition of picosecond laser microstructured aluminum in ambient air, J. Colloid Interf. Sci. 441 (2015) 1-9.

The authors greatly appreciate editor's and reviewer's time and efforts dedicated to our paper. This paper will be of great interest to readers who concentrate on laser-induced wettability transition mechanism. We hope that in light of our responses to the comments, our revised manuscript can be acceptable for publication in ***Progress in Organic Coatings***.

Yours sincerely,

Yanling Tian

School of Engineering

University of Warwick, Coventry CV4 7AL, UK

Email: meytian@tju.edu.cn, Y.Tian.1@warwick.ac.uk

Highlights:

1. A super-hydrophobic surface was fabricated by hybrid technique of laser ablation and fluoroalkylsilane modification.
2. The super-hydrophobic coating can anchor lubricating oil to obtain slippery coating.
3. Saline water can clean fluoride components upon the super-hydrophobic surface.
4. The slippery coating presented superior anticorrosion performance to super-hydrophobic coating.

Graphical abstract:

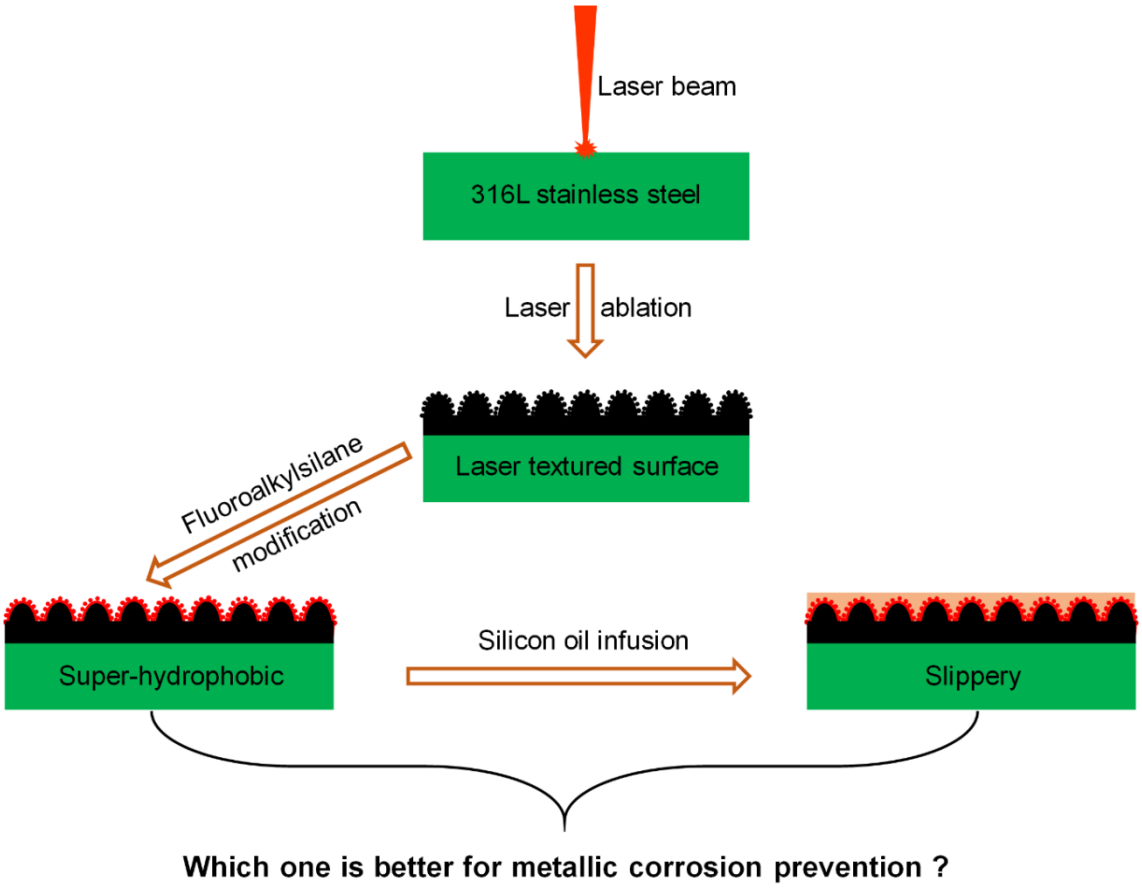

A contrastive investigation on anticorrosive performance of laser-induced super-hydrophobic and oil-infused slippery coatings

Zhen Yang, Xianping Liu, Yanling Tian*

School of Engineering, University of Warwick, Coventry CV4 7AL, UK

*Corresponding author e-mail address: meytian@tju.edu.cn, Y.Tian.1@warwick.ac.uk

Abstract

Nature inspired super-hydrophobic surface has aroused extensive attention on corrosion prevention. More works have investigated the instant corrosion resistance of fresh super-hydrophobic surface, but less research focused on its stability when immersed into corrosive solution for long time. Recently, another bio-mimic surface with slippery coating also presented great corrosion inhibition due to its excellent insulation between the corrosive medium and base material. However, which coating is suitable for long-term immersion into corrosive environments still remains to investigate. Herein, we firstly fabricated a super-hydrophobic coating on 316L stainless steel by nanosecond laser ablation combining fluoroalkylsilane modification. Then a slippery coating was obtained by further infusing silicon oil into the as-prepared super-hydrophobic substrate. The PDP and EIS measurements indicate that both fresh super-hydrophobic and slippery surface were observed to improve the corrosion inhibition for the base substrate, and the performance of slippery surface was superior to that of super-hydrophobic surface. Immersion experiments infer that the air cushion of the super-hydrophobic surface was easily destroyed, resulting in a rapid failure of super-hydrophobicity and instability of corrosion resistance. In contrast, after immersed into 3.5 wt.% NaCl solution, the wetting property of oil-impregnated slippery surface almost remained the same. In addition, the electrochemical measurements reveal that the slippery coating presented exceptional anticorrosion behavior after long-term immersion into corrosive liquid. Therefore, the authors believe this study is expected to promote the development of anticorrosive coating for the steel materials. This work is of great importance for employing laser ablation to fabricate slippery surface, which is convenient and effective for metallic corrosion prevention in industrial fields.

Keywords: Laser ablation; Super-hydrophobic; Oil-infused slippery; Corrosion prevention; Stability

1. Introduction

Corrosion costs more than US$ 4 trillion annually in the world [1]. The degradation of metals by chemical and electrochemical reactions is ubiquitous, causing detrimental consequences of global economic losses, ecological system and potential safety issues [2]. As one of the most common materials in our daily life, stainless steel has a wide range of applications including three dominant areas: construction, manufacturing and automotive sectors. It is reported that stainless steel is susceptible to pitting corrosion in humid and salty conditions as well as harsh chemical environments, particularly in the corrosive solutions containing halide ions [3-4]. Thus, the corrosion resistance and stability of stainless steel become the critical concerns in engineering applications. One of the conventional methods to prevent corrosion is the usage of protective coatings, such as organic coating [5], polymeric coating [6], graphite coating [7], Ni-P coating [8], and ceramic coating [9]. However, the first three mentioned coatings could not maintain long-term stability when exposed to salty corrosive liquids, due to the poor adhesion to steel surface. Although the Ni-P coating and ceramic coating can enhance corrosion resistance of steel substrate to some extent, it is far from the goal due to the presence of surface pores or surface cracks formed during the fabrication process. Though the surface pores and cracks, the corrosive media would directly contact the pristine steel substrate, resulting in localized corrosion at coating/substrate interface. Therefore, more alternative strategies should be exploited to mitigate the corrosion reactions, and further improve the anticorrosive performance of steel for long-term stability.

Recently, inspired by nature, previous literature reported that the application of super-hydrophobic coating can be regarded as an effective route for corrosion prevention due to its splendid low-affinity to water [10-13]. At present, various techniques have been used to successfully fabricate super-hydrophobic coatings, such as thermal embossing [14], chemical etching [15], chemical vapor deposition [16], electrodeposition [17], sol-gel [18], and hydrothermal reaction [19], etc. However,

above methods generally involve tedious chemical preparation, multiple processing steps and expensive equipment, which will limit the fabrication efficiency for super-hydrophobic products [20]. On the contrary, laser surface texturing is recently regarded as a convenient and green approach to produce super-hydrophobic surfaces because it can create micro/nano structures with high processing accuracy and low thermal damage [21]. In addition, through precise control of laser parameters, stable three dimensional (3D) hierarchical surface texture can be obtained without polluting environment. Previous research proved that two kinds of laser-processing can be used to produce super-hydrophobic surfaces. The first one is purely based on laser-induced rough micro/nano structures [22], and the other is based on laser processing and fluoroalkylsilane modification [23-24]. When these super-hydrophobic surfaces were immersed into corrosive solutions, the contact area at the solid/liquid interface will be remarkably minimized based on the entrapped air pockets, which serve as the soft barriers to prohibit corrosive species [25]. During the initial immersion period into simulated seawater, a great number of previous studies have demonstrated that the corrosion resistance could be firmly improved by applying super-hydrophobic coating as a barrier layer. However, the report is limited on long-term stability of super-hydrophobic coating when immersed into corrosive solution. There is no doubt that the air cushion is metastable, and the thin air film may exhibit a decay due to water pressure and long-term immersion. The limited stability of air layer will result in the deterioration of surface anticorrosive performance, explaining the rarity of submersed super-hydrophobic surface for commercial applications [26].

Motivated by nature again via mimicking *Nepenthes* pitcher plant, slippery surface is considered as an admirable paradigm of protective coating by infusing intermediary phase (also called lubricating oil) as liquid cushion to replace the unstable air layer [27]. Different from super-hydrophobic surface, the slippery surface employs rough micro/nano structures to store the lubricating silicon oil rather than the air pockets. The infused oil can be strongly anchored in the micro/nano structures with the assistance of capillary effect and Van der Waals force [28-30]. Three criteria should be considered to successfully fabricate the slippery surfaces: (1) the substrate must have space and

vacancy to host the lubricating liquids; (2) it should be immiscible between the lubricating and the external liquids; (3) the substrate should be firstly wetted by lubricating liquids instead of the liquids to be repelled [31]. The as-prepared slippery surface is proved to present excellent water-repealing property due to its low affinity to water phase. Therefore, slippery coating is also a prominent alternative for metallic protection because of its exceptional lubricating barrier to inhibit the corrosive media contacting the base substrate [32-33]. In addition, it is intriguing that the as-prepared slippery coating has self-healing character in the light of inherent mobility of lubricating oil film, which endows the slippery system with distinguished corrosion resistance. Compared with super-hydrophobic surface, the damaged spots on oil-infused slippery surface could be spontaneously recovered in a short time, leading to the restriction of corrosion propagation. To the best of author's knowledge, the fabrication of super-hydrophobic surface has lasted more than one decade, but in contrast, little research has been focused on the stability of its anticorrosive performance. On the other hand, the investigation on corrosion inhibition of slippery surface is greatly less. Thus, more attention should be paid on the fabrication of slippery surface in order to find alternative strategy for corrosion mitigation.

This work firstly fabricated a super-hydrophobic coating upon stainless steel by hybrid processes of nanosecond laser ablation and fluoroalkylsilane modification. A slippery coating was obtained through a consecutive operation involving infusion of lubricating silicon oil. As a versatile platform, the super-hydrophobic surface not only presented good corrosion resistance, but also served as an anchoring site for lubricating oil. In terms of anticorrosive performance, a comparison between the newly fabricated super-hydrophobic surface and slippery surface was carried out utilizing potentiodynamic polarization (PDP) and electrochemical impedance spectroscopy (EIS) measurements to explore which kind of coating is the better option for corrosion prevention. Then they were immersed into 3.5 wt.% NaCl solution for different time. The wettability evolution implies that the super-hydrophobic coating was not stable, and its anticorrosive performance would considerably decline due to the deterioration of air cushion and penetration of corrosive ions (Cl^-) into the pristine substrate. On the

contrary, the slippery surface can maintain excellent stability after immersed into corrosive solution for 72 hours. The following PDP and EIS experiments indicate that the corrosion behavior of slippery surface did not change much. Therefore, the corrosion resistance of the oil-infused slippery surface was superior to that of the super-hydrophobic surface in harsh conditions. It can be expected that based on the addition of fluoroalkylsilane modification and silicon oil coating, stainless steels can be more suitably utilized in sewage pipeline, marine vessel, underground and submarine cables, etc.

2. Experimental

2.1. Materials and chemicals

316L stainless steel with dimension of 30 × 10 mm^2 and thickness of 1mm was investigated in this work. The samples were mechanically polished, then ultrasonically washed in sequence with acetone, ethanol and distilled water each for 10 minutes to eliminate surface pollutants. The rinsed samples were dried by the compressed nitrogen gas. All the chemicals and reagents (AR) including sodium chloride, silicon oil, and 1H, 1H, 2H, 2H-perfluorodecyltriethoxysilane (FAS) were purchased from Alfa Aesar Company, used as received without further purification. Distilled water was produced by a commercial water purification system and utilized in all experimental procedures.

2.2. Nanosecond laser ablation

An Ytterbium nanosecond fiber laser (IPG Photonics, Germany) was employed to create the unique surface texture. This laser machine can emit 1064 nm-center-wavelength pulses with a repetition rate of 20 kHz and a duration of 50 ns. The as-prepared substrates were mounted on a fixed platform. The laser beams were focused upon the 316L steel substrates with a spot diameter of 50 μm. The laser power and laser scanning speed were 10 W and 500 mm/s, respectively. The substrates were ablated in two perpendicular directions by the moving laser beams via line-by-line scanning strategy with the shift of scanning lines at 60 μm, which resulted in the grid-patterned structures. More details of the laser ablation procedure can be found in our previous papers [34-37].

2.3. Fabrication of super-hydrophobic surface and oil-infused slippery surface

Posterior to the laser ablation, a hierarchical micro/nano structure was generated on 316L steel substrate. During the ablation process, it is observed that many ash residues were produced. Therefore, the laser-induced sample was firstly flushed by distilled water and then blown by compressed nitrogen gas in order to remove surface contaminants. Here, the initial laser-processing surface was obtained. Then they were immersed into the uniform FAS/ethanol solution (containing 0.5 g FAS, 62.8 mL ethanol and 19.2 mL distilled water) for 2 hours to lower surface free energy. After flushed by distilled water and heated in oven at 110 ℃ for 1 hour, the super-hydrophobic 316L steel surface was obtained.

Subsequently, excess 100 cSt silicon oil was dripped on the laser-induced super-hydrophobic sample. The silicon oil can be infused into the laser-induced hierarchical structures and locked into the laser ablated pits and vacancies. Then, the oil-infused super-hydrophobic surface was vertically placed for one night to get rid of the excess oil. Eventually, the slippery coating was achieved upon the super-hydrophobic surface due to the storage of the lubricating oil film. For reference, a pure 316L stainless steel substrate was also treated with silicon oil and then processed with the same method as slippery surface, called pristine surface with oil.

2.4. Characterization

The surface topography of the nanosecond laser-induced 316L sample was observed using scanning electron microscopy (SEM, Quanta 250 FEG, FEI, America) which is equipped with energy-dispersive spectroscopy (EDS, X-Max 80, Oxford Instruments). Water contact angle (WCA) and sliding angle (SA) were measured with an 8 μL distilled water droplet at the cleanroom condition using a contact angle goniometer (VCA optima, AST Products, America). Five different spots on each surface were measured to determine the average WCA and SA. The surface chemical compositions of the pristine and super-hydrophobic surface were analyzed by X-ray photoelectron spectroscopy (XPS, Escalab 250Xi, Thermo Fisher Scientific, America). CasaXPS software was utilized to interpret the XPS data.

The corrosion tests were performed at cleanroom temperature by an electrochemical workstation (660D, CH Instruments, Inc., China), and 3.5 wt.% NaCl

aqueous solution as corrosive solution. A standard three-electrode cell configuration consisted of a saturated calomel reference electrode (SCE) and a platinum counter electrode. Pristine 316L steel substrate, initial laser-processing surface, pristine surface with silicon oil, super-hydrophobic surface and slippery surface were in turn served as the working electrode with 1 cm^2 exposed area in the corrosive solution. In order to make the system stabilize, the samples were soaked into the corrosive medium for 30 minutes before the electrochemical measurements. The scanning rate was set at 10 mV/s for the PDP tests. The EIS experiments were performed within the frequency scope from 100000 to 0.01 Hz, and a sinusoidal signal amplitude of 10 mV.

3. Results and discussion

3.1. Surface morphology and chemical compositions

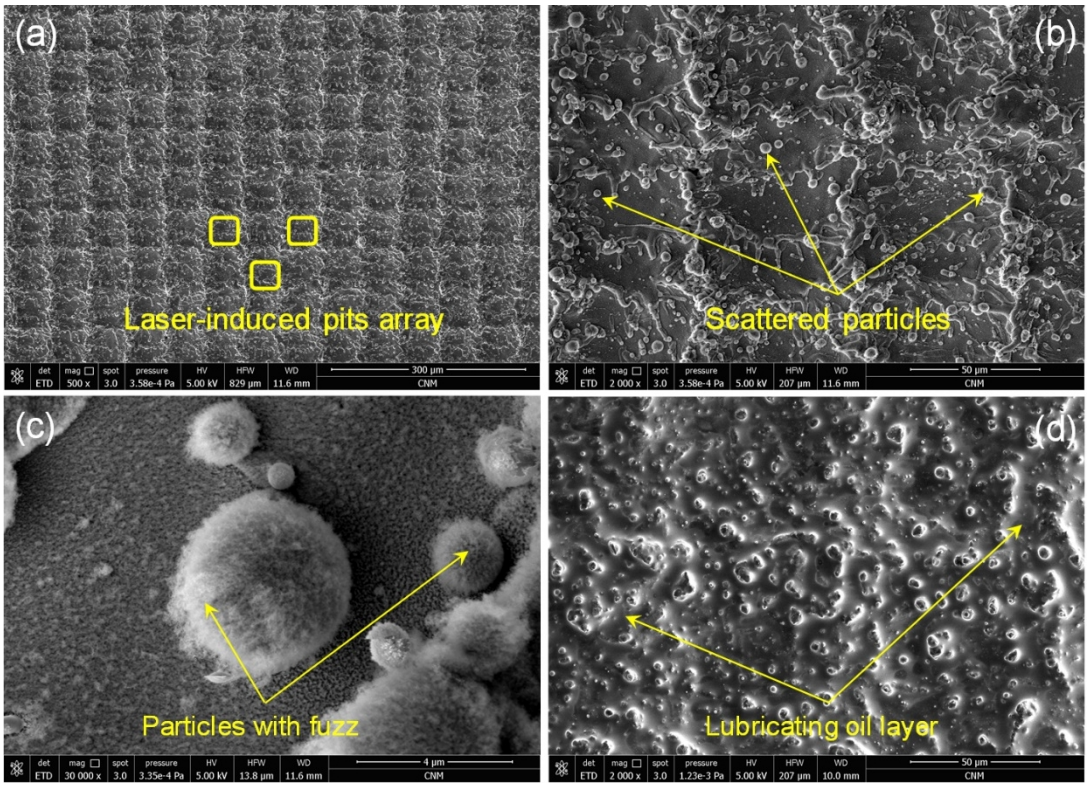

Figure 1. (a-c) SEM images of the laser-induced 316L steel surface with various scale bar and (d) the SEM image of the slippery surface.

Figs. 1a-c show the SEM images with different magnifications for the laser-induced super-hydrophobic surface. It can be seen from Fig. 1a that the laser-induced surface presented a hierarchical structure with micro-scaled pits array. The detailed image of Fig. 1b reveals that an abundance of particles was scattered on the as-prepared

surface. This is because during the laser ablation process, the interfacial materials will be removed and ejected over the sample. The sputtered substance was in the form of molten particles with micro or nano size. Once these particles fell back and re-solidified onto the sample surface, the laser-induced surface was covered with the micro/nano-scaled particles. As shown in Fig. 1c, the created particle was complex, and it was covered with nano-scaled fuzz. It can be concluded that the laser-induced surface consisted a robust hierarchical structure, which is an important element for the super-hydrophobicity due to the formation of more space to trap air. It is noted from Fig. 1d that the surface structure for the slippery surface is different from the surface texture of the super-hydrophobic surface. SEM image indicates that the laser ablated pits can be served as the vacancies and host the lubricating silicon oil. Part of the gap was filled, forming a lubricating oil layer. However, the slippery surface also presented a hierarchical structure although the silicon oil was injected into the composite texture. Similar topography of the slippery surface can be found in the previous literature [38]. Therefore, the laser-induced hierarchical structures with pits array and particles can offer an air cushion to obtain super-hydrophobicity and anchor the silicon oil to achieve the slippery property.

Compared with the pristine 316L steel substrate, the modifications of surface chemistry regarding to the as-prepared super-hydrophobic sample were investigated by XPS technique. The corresponding wide scan spectra and high-resolution spectrum of C 1s are displayed in Fig. 2. It is obvious from Fig. 2b that two distinct elements of F and Si were observed on the super-hydrophobic surface, indicating that the FAS molecules were grafted on the laser-induced sample during the immersion period into the FAS/ethanol solution. In order to further validate this hypothesis, the C 1s spectrum was decomposed, and the curve-fitted spectrum consisted of seven peak components. The peak signals at the binding energy of 284.7 eV, 286.3 eV and 288.1 eV were due to the presence of C-C(H), C-O and O-C=O bond, respectively. The peaks centered at 290.2 eV, 291.1 eV and 293.3 eV were attributed to the functional groups of CH_2-CF_2, -CF_2 and -CF_3, respectively. In addition, the C-Si bond was also detected locating at the 283.9 eV [39]. The detected fluoride functional groups were definitely originated

from the FAS molecules, resulting in the formation of super-hydrophobicity for the laser-induced surface due to the dramatic reduction of surface free energy [40]. Therefore, it can be summarized that the synergistic effects of laser-induced hierarchical structure and the presence of low free energy functional groups contributed to the as-prepared super-hydrophobic surface.

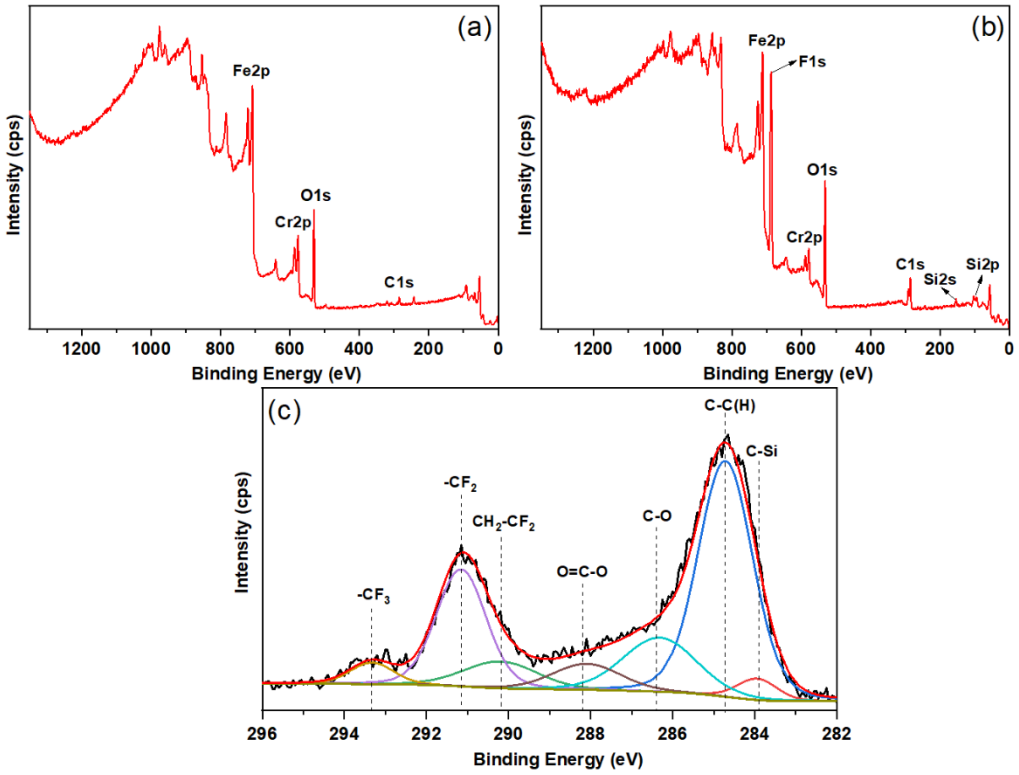

Figure 2. XPS wide scan spectra of (a) pristine 316L steel and (b) super-hydrophobic surface, (c) C 1s high-resolution spectra of the super-hydrophobic surface.

In order to fabricate slippery surface, silicon oil is an ideal candidate due to its eco-friendly and nonvolatile properties. Then, silicon oil was dripped on the fluoride-modified super-hydrophobic surface with hierarchical structures. The lubricating oil will wet and fill into the laser-induced pits array due to the strong adhesion to the super-hydrophobic surface under capillary effect and Van der Waals force [41-43]. To conclude, the slippery surface can be obtained after the laser-induced surface was firstly modified with silanization process, and then infused with lubricating silicon oil.

3.2. Surface wettability

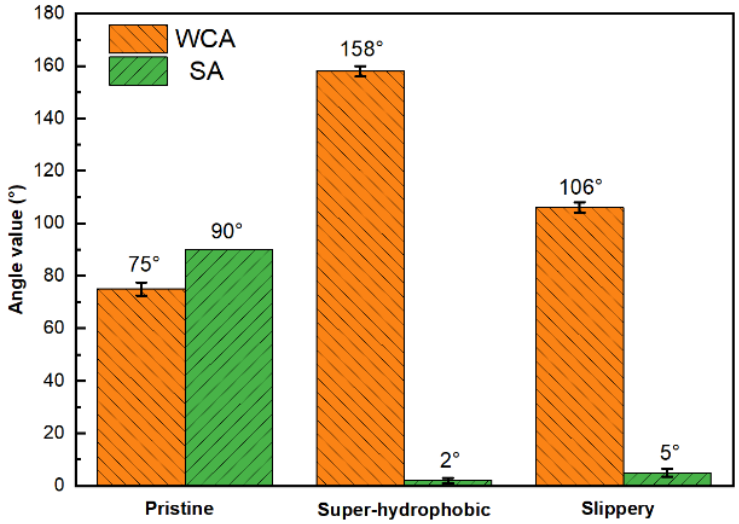

Figure 3. WCA and SA values for the pristine, super-hydrophobic and slippery surface.

The wetting properties of the pristine steel substrate, as-prepared super-hydrophobic and oil-impregnated slippery surface were evaluated by the WCA and SA measurements. Fig. 3 shows that the pristine surface presented intrinsic hydrophilicity with a WCA value of 75 ± 3º. In terms of SA, even if the steel substrate was vertically placed or turned over, the water droplet was confirmed to stick upon the substrate. This phenomenon is ascribed to the high adhesion force between the water droplet and the substrate surface, and the droplet cannot freely leave the pristine steel material. Posterior to the hybrid laser ablation and FAS immersion process, the fabricated surface showed a super-hydrophobic character with a WCA value of 158 ± 2º. It can be seen from Movie S1 (Supporting Information) that the water droplet can easily roll off the super-hydrophobic surface, demonstrating a very small SA value of 2 ± 1º. The formation of super-hydrophobicity could be attributed to much more air pockets entrapped into the rough hierarchical structures and the surface energy reduction by the modification of fluoride components. The slippery surface was obtained by injecting the lubricating oil into the fluorosilane-modified rough structures, which maintained the hydrophobic behavior with the WCA of 106 ± 2º. Similar with the super-hydrophobic surface, the slippery surface modified by silicon oil also showed excellent water repellent character. As shown in Movie S2 (Supporting Information), the water droplet can easily slide down the oil-infused slippery surface when the inclination angle of the sample was lowered to 5º. The formation of a lubricating layer can repel the water

droplets to slide downward. The silicon oil can be effectively retained in the laser-induced pits array and vacancies, which was due to the capillary effect, Van der Walls force as well as the gravity effect [44]. In addition, the hydrophobicity of the initial laser-processing surface and the pristine 316L substrate with silicon oil coating were also evaluated for comparison. It is noted from Fig. S1 (Supporting Information) that the water droplet will quickly spread upon the initial laser-processing surface, presenting an extremely small WCA (almost 0°). For the flat substrate with silicon oil coating, its WCA value was measured at 91 ± 5º that was lower than the as-prepared slippery sample. The reason may lie in the absence of laser-induced micro/nano structures and the following silanization treatment.

3.3. Anticorrosion performance

The 316L stainless steel are widely used in industries, and it is highly susceptible to corrosion. The preparation of a protective coating upon the steel surface may be one of the most effective strategies to prohibit corrosion reactions. A super-hydrophobic coating and an oil-impregnated slippery coating prepared on pristine steel surface were measured by PDP and EIS in 3.5 wt.% NaCl solution. For reference, the pristine substrate, initial laser-processing surface, and the pristine surface with silicon oil coating were also explored. Especially, the instant anticorrosion performance of the as-prepared super-hydrophobic and slippery coatings was compared. Subsequently, the stability of the two kinds of coatings was evaluated under different immersion time into corrosive solution.

3.3.1. Corrosion resistance of the newly fabricated surfaces

PDP tests and EIS experiments were carried out on the newly fabricated super-hydrophobic surface and slippery surface as well as the reference samples to evaluate the anticorrosion behavior, and the 3.5 wt.% NaCl solution was prepared to be the corrosive liquid. The received PDP curves of the investigated samples were depicted in Fig. 4. The extrapolation method of Tafel plots was used to interpret the corrosion parameters, and the fitting results are summarized in Table 1.

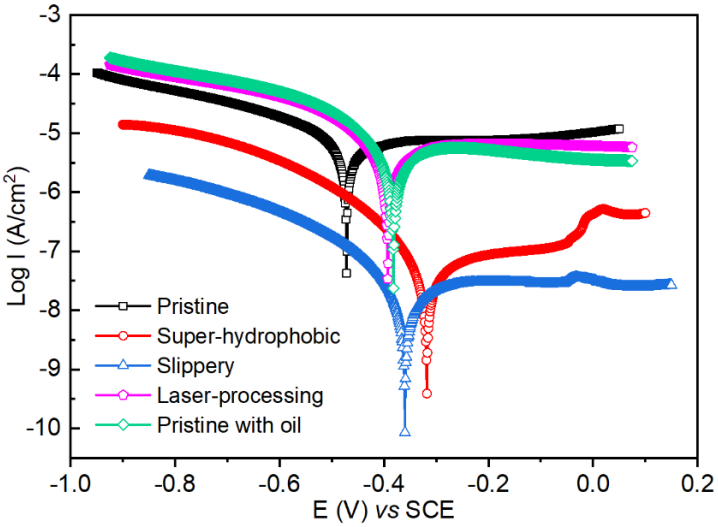

Figure 4. PDP curves for the studied samples.

Table 1. Fitting results of the investigated samples derived from PDP curves.

Sample	E_{corr} (V)	I_{corr} (A/cm^2)	β_a (V/dec)	$-\beta_c$ (V/dec)	R_p (kΩ cm^2)
Pristine	-0.443	4.56×10^{-6}	0.332	0.239	13.23
Laser-processing	-0.385	2.37×10^{-6}	0.352	0.152	19.46
Pristine with oil	-0.378	2.09×10^{-6}	0.382	0.134	20.61
Super-hydrophobic	-0.312	4.70×10^{-7}	0.402	0.116	83.16
Slippery	-0.356	1.61×10^{-8}	0.446	0.107	2327.42

In general, better corrosion resistance behavior can be reflected by the lower corrosion current density (I_{corr}) and more positive corrosion potential (E_{corr}) because the actual corrosion rate can be revealed by corrosion current density [43], and the polarization resistance (R_p) is inversely proportional to the corrosion current density and directly proportional to the corrosion potentials [45]. It is noted from Fig. 4 that compared with the pristine substrate, the Tafel plots of the fresh super-hydrophobic and slippery surface experienced the simultaneous downward and rightward shift, indicating a decreased corrosion current density (I_{corr}) and a positive shift of corrosion potential (E_{corr}). Hence the pristine steel substrate could be protected by the super-hydrophobic or slippery coating. As shown in Table 1, the fitting results clearly demonstrate that the slippery surface possessed the lowest corrosion current density I_{corr} (1.61×10^{-8} A/cm^2), around 30-fold smaller than the super-hydrophobic surface (4.70×10^{-7} A/cm^2) and 300-fold smaller than the pristine substrate (4.56×10^{-6} A/cm^2). The results infer that the slippery and super-hydrophobic coatings can lower the corrosion

current density and inhibit corrosion reactions, being it from the lubricating oil layer and the entrapped air pockets among the laser-induced micro/nano structures with pits array. In terms of the initial laser-processing surface and the pristine surface with silicon oil, they presented similar positive shifts of corrosion potential and decreased trends of corrosion current density compared with the pure stainless steel, showing an improvement of corrosion resistant behavior. Previous report proved that the oxidation layer (Fe_2O_3 and Gr_2O_3) formed during the laser ablation treatment could inhibit the corrosion reactions for the laser-processing surface [46]. Furthermore, as an insulating layer, the silicon oil coating on the pure 316L surface can also improve the corrosion resistance to certain degree. However, the fitting data in Table 1 obviously indicate that the anticorrosion performance of the as-prepared slippery and super-hydrophobic surfaces was greatly enhanced than the laser-processing surface and the pristine surface with silicon oil, and the slippery surface presented the best anticorrosive behavior among the five studied samples. In addition, the polarization resistance (R_p) of the investigated samples were determined by Stern-Geary formula as shown below:

$$R_p = \frac{\beta_a \times \beta_c}{2.303 I_{corr}(\beta_a + \beta_c)} \quad (1)$$

where the Tafel slops of the anodic and cathodic plots are denoted as β_a and β_c, respectively. The calculated R_p values displayed in Table 1 obey the following sequence: slippery surface (2327.42 kΩ cm^2) > super-hydrophobic surface (83.16 kΩ cm^2) > pristine surface with silicon oil (20.61 kΩ cm^2) > laser-processing surface (19.46 kΩ cm^2) > pristine substrate (13.23 kΩ cm^2), revealing that the anticorrosive performance of the oil-infused slippery surface was superior to that of the super-hydrophobic surface, and the reference samples.

Among the five investigated samples, the as-prepared slippery surface showed the best anticorrosive property based on the presence of micro/nano structures and lubricating oil layer, which can be further confirmed by the powerful EIS technique. Figs. 5a and 5b depict the Nyquist plots of the pristine substrate, the fresh super-hydrophobic and slippery sample measured in the corrosive NaCl solution. Previous works prove that the variation of charge transfer resistance during corrosion process

results in significant difference of the capacitance loop, and the surface coating will perform better corrosion resistance if its Nyquist plot presents a larger axial radius of semi-elliptical arc [47]. It is noted that compared to the pristine steel substrate, the fresh super-hydrophobic and slippery coatings had widespread capacitive loops, indicating that the corrosive ions (Cl^-) in electrolyte were difficult to touch the bare substrate. Therefore, the fresh slippery surface presented the best corrosion resistance due to its largest capacitive loop, followed by the fresh super-hydrophobic surface. In addition, the Bode plot of impedance modulus vs frequency (as shown in Fig. 5c) was used to continue the exploration. In the low frequency, it is obvious that the fresh slippery surface had the highest value of impedance modulus |Z| ($10^{5.58}$ Ω cm^2), greater than the fresh super-hydrophobic surface ($10^{4.76}$ Ω cm^2) as well as the pristine substrate ($10^{3.19}$ Ω cm^2). As shown in Fig. S2 (Supporting Information), the pristine surface with silicon oil and laser-processing surface showed similar EIS plots. Although the Nyquist loop diameters of these two samples were larger than the pristine substrate, such diameters were greatly smaller than the as-prepared slippery surface and super-hydrophobic surface. Besides, the impedance modulus |Z| in the low frequency of pristine surface with oil and laser-processing surface were only $10^{4.36}$ Ω cm^2 and $10^{4.27}$ Ω cm^2, respectively. Therefore, the above results infer that the oil-infused slippery coating can retard the generation of corrosion products, further confirming that the fresh slippery surface exhibited the best corrosion resistance compared with the newly fabricated super-hydrophobic surface and other reference samples.

The corresponding equivalent circuit models were proposed to fit the EIS plots, as shown in the inserted diagrams of Figs. 5a and 5b, in which R_s denotes the solution resistance. In order to obtain the best-fit impedance plots, the constant phase element (CPE) is utilized to simulate the capacitance. The following mathematical equation is used to describe the impedance of CPE component [48]:

$$Z_{CPE}=[Q\,(jw)^{\alpha}]^{-1} \quad (2)$$

where Q represents proportionality factor (unit: $10^{-5}\Omega^{-1}s^{n}cm^{-2}$), j denotes the imaginary unit, and angular frequency is depicted by w. The exponential coefficient α lies between

0 and 1 [49]. R_{ct}||CPE_{dl} components mean the charge transfer resistance and electrical double layer capacitance between the substrate and the coating. R_f||CPE_f elements denote the resistance and capacitance due to the super-hydrophobic or slippery coating.

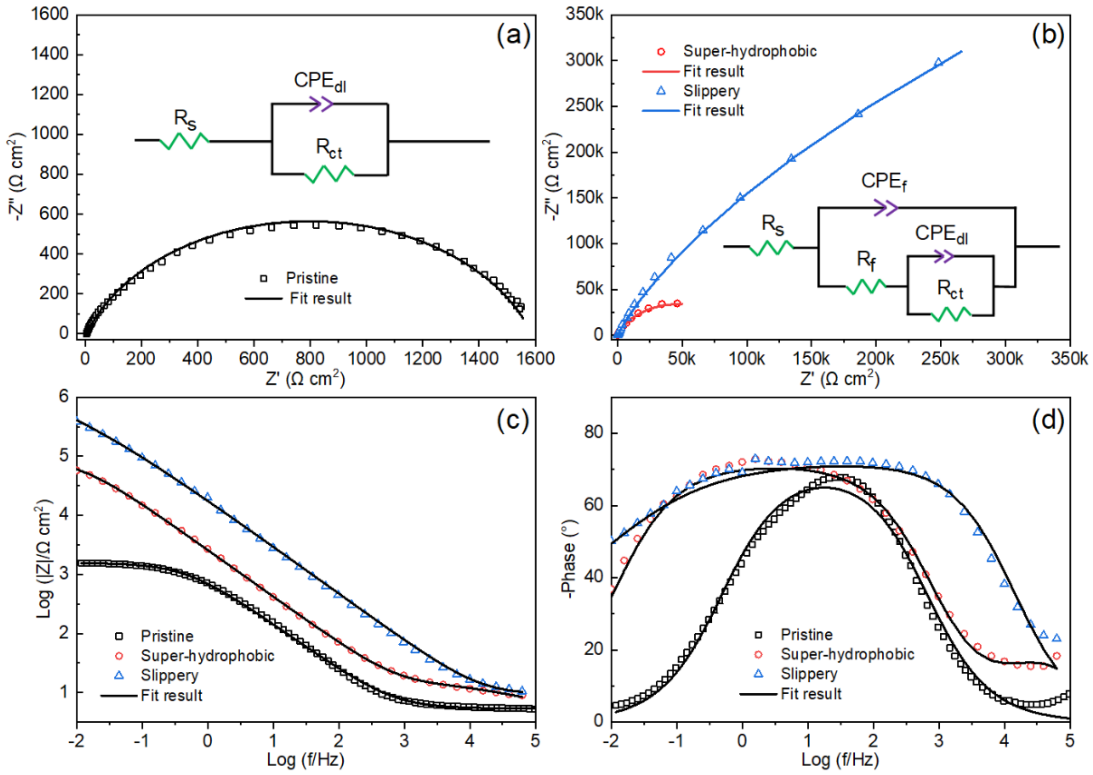

Figure 5. Nyquist plots of (a) the pristine substrate and (b) the fresh super-hydrophobic and slippery surface; the inserts are their corresponding equivalent circuit models; Bode plots of (c) |Z| vs frequency and (d) phase angle vs frequency for the three studied samples.

The simulated electrochemical corrosion parameters are summarized in Table S1 (Supporting Information). The R_{ct} value is generally used to reveal the corrosion resistant performance, and larger R_{ct} value means the charge transfer reaction is more sluggish [50]. The fitted parameters show that the R_{ct} value of the fresh slippery surface can reach up to 10300 kΩ cm^2, compared with the fresh super-hydrophobic surface 95.32 kΩ cm^2, pristine surface with silicon oil 33.51 kΩ cm^2, laser-processing surface 23.56 kΩ cm^2, and the pristine 316L steel substrate 1.58 kΩ cm^2. The results indicate that the slippery and super-hydrophobic surface can significantly retard the generation of corrosion products and thus improve the protective performance for the bare substrate. The reasons are that the lubricating silicon oil is immiscible to water, and it can be firmly anchored to the laser-induced hierarchical structures as an insulating layer.

Besides, the corrosion resistance of the super-hydrophobic surface can be attributed to the formation of air cushion that can repel the corrosive medium to reach the bare substrate. The fitted EIS parameters were in good agreement with the PDP results, clearly revealing that the corrosion inhibition efficiency of the oil-infused slippery surface is much better than that of the super-hydrophobic surface and the reference samples.

3.3.2. Corrosion resistance with immersion time

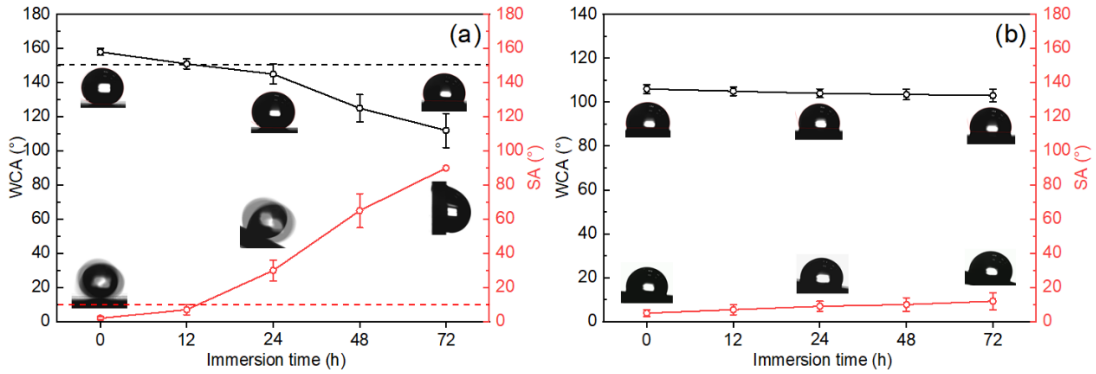

Figure 6. The evolution of WCA and SA for (a) super-hydrophobic surface and (b) slippery surface with the increasing immersion into 3.5 wt.% NaCl corrosive solution.

The stability of the protective coating immersed into corrosive environment is a critical indicator for the practical applications in corrosion inhibition of metals. In this work, the as-prepared super-hydrophobic and slippery surfaces were soaked in the 3.5 wt.% NaCl solution for 12, 24, 48 and 72 hours to explore their corrosion resistant stability. Fig. 6 shows the evolution of WCA and SA for the super-hydrophobic and slippery surfaces under different immersion time, and the detailed values of contact angles are presented in Table S2 (Supporting Information). From Fig. 6a, it is easy to find that the WCA of as-prepared super-hydrophobic surface continuously decreased, while the SA increased with the increasing of immersion time. Within 12 hours immersion into NaCl solution, the immersed surface could maintain super-hydrophobicity with WCA greater than 150º and SA less than 10º. When the immersion time was prolonged to 24 hours, it would loss its super-hydrophobicity, showing a hydrophobic property. After 72 hours immersion treatment in corrosive solution, the water droplet was strongly stuck on the immersed surface even if the sample was vertically positioned. It can be deduced that the air pockets entrapped in the rough

hierarchical structures was unstable and the corrosive liquid would gradually penetrate in the formed air cushion, leading to more surrounding corrosive liquids directly contacting the super-hydrophobic surface. Long-term exposure to the corrosive solution, the corrosion resistance of the super-hydrophobic surface will be weakened due to the presence of surface cracks [51]. Through cracks, the penetration of harmful ions could directly contact the bare substrate, leading to the formation of corrosion products. After long-term immersion, the protective coating will be damaged due to the localized corrosion attack. Therefore, the laser-induced super-hydrophobic surface with rough surface structure cannot present long-term stability of corrosion resistance.

Apart from the surface structure, the surface chemistry was also examined on the super-hydrophobic surfaces under different immersion time. Figs. 7a-e show the EDS spectra and weight percentage of main elements on the immersed steel substrates. It is interesting to find that the fluorine content experienced a continuous decrease with the increase of immersion time into corrosive NaCl solution, which can be clearly proved by Fig. 7f depicting the changes of fluorine content. The results indicate that the saline water containing harmful ions could clean the fluoride components, leading to the increase of surface free energy and the loss of super-hydrophobicity. Based on the above analyses, it can be concluded that both the surface structure and surface chemical components play important role in the change mechanism of anticorrosive performance when the super-hydrophobic surfaces were immersed into corrosive solution for long time. The unstable air cushion would be destroyed, and then the surrounding harmful ions could erode the laser-induced surface structure, resulting in the generation of surface cracks. Through cracks, the harmful ions could directly contact the base material, leading to the failure of corrosion resistance. From the perspective of surface chemical components, the saline water can remove the fluoride components. The reduction of fluorine content would result in the loss of super-hydrophobicity as well as anticorrosive performance.

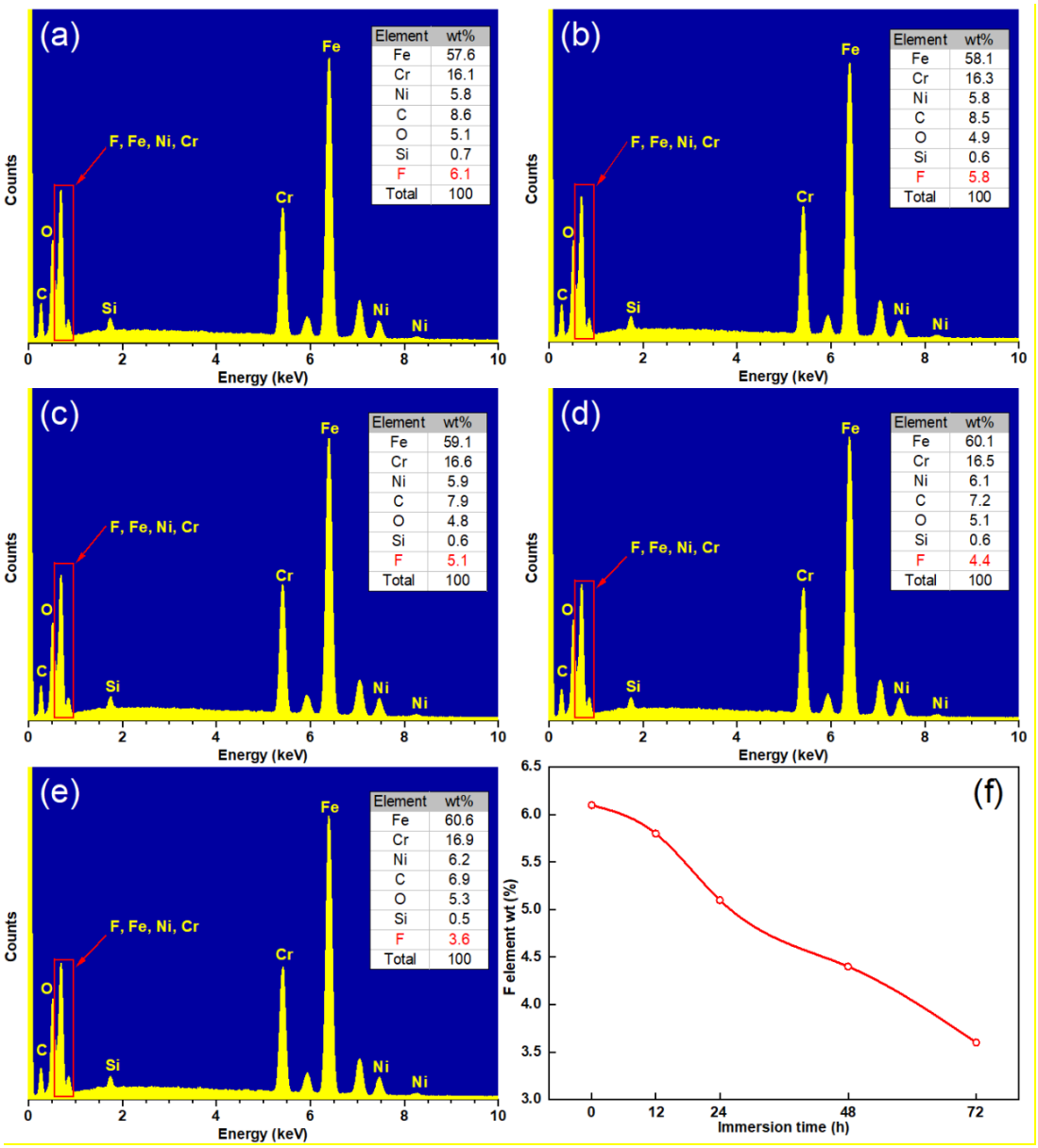

Figure 7. EDS spectra of the as-prepared super-hydrophobic surfaces after immersion into NaCl solution for (a) 0 h, (b) 12 h, (c) 24 h, (d) 48 h, (e) 72 h; (f) the changes of fluorine content with immersion time.

In contrast, the fabricated slippery surfaces were also immersed into 3.5 wt.% NaCl solution, and their WCA and SA values depicted in Fig. 6b show significant difference from the contact angle values of the super-hydrophobic surfaces. The contact angle measurements indicate that within 72 hours, the WCA values of the slippery surfaces almost remained the same at around 105º. Although the SA was observed a slight increase, the water droplet can still slide down the sample surface at around 12º, exhibiting excellent water repealing property. The contact angle evolution implies that

the lubricating oil layer on the slippery surface can be stably locked in the hierarchical structures due to the capillary effect and Van der Waals force, which can be served as a perfect insulator to corrosive liquid.

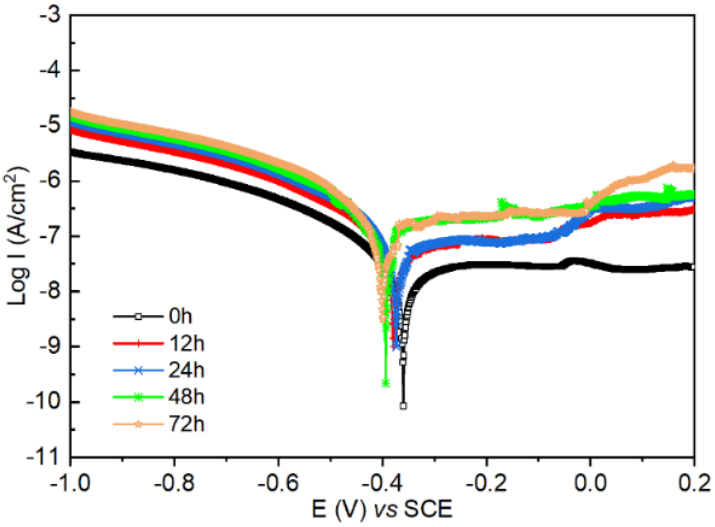

Figure 8. PDP curves of the as-prepared slippery surfaces with different immersion time into 3.5 wt.% NaCl solution.

Table 2. Fitted corrosion parameters of the slippery surface immersed into NaCl solution for 12, 24, 48, and 72 hours.

Sample	E_{corr} (V)	I_{corr} (A/cm^2)
Slippery (0 hour)	-0.356	1.61×10^{-8}
After 12 hours	-0.358	4.40×10^{-8}
After 24 hours	-0.361	5.10×10^{-8}
After 48 hours	-0.365	1.04×10^{-7}
After 72 hours	-0.371	1.35×10^{-7}

Furthermore, the anticorrosive stability of the slippery sample with different immersion time was explored by electrochemical measurements. After immersed in 3.5 wt.% NaCl solution for certain hours (0, 12, 24, 48, and 72 hours), the corresponding PDP curves are depicted in Fig. 8. The fitted corrosion parameters are shown in Table 2. The results reveal that with prolonged period of immersion, the corrosion potential (E_{corr}) of the slippery surface did not change much posterior to 72 hours immersion and finally shifted to -0.371 V, showing a good corrosion resistant stability in corrosive liquid. The corrosion current density (I_{corr}) slightly increased, which may be attributed to the slight decrease of oil layer thickness. If the lubricating oil layer became thinner,

the corrosive media could penetrate in the interface of substrate/coating easier [52]. However, even when the slippery surface was immersed into corrosive NaCl solution for 72 hours, its corrosion current density was 1.35×10^{-7} A/cm^2, still more than 3 times lower than the newly fabricated super-hydrophobic surface (4.56×10^{-6} A/cm^2) and about 34 times smaller than the pristine steel substrate (4.70×10^{-7} A/cm^2). Therefore, the slippery surface was proved to present a superior stability of anticorrosive performance.

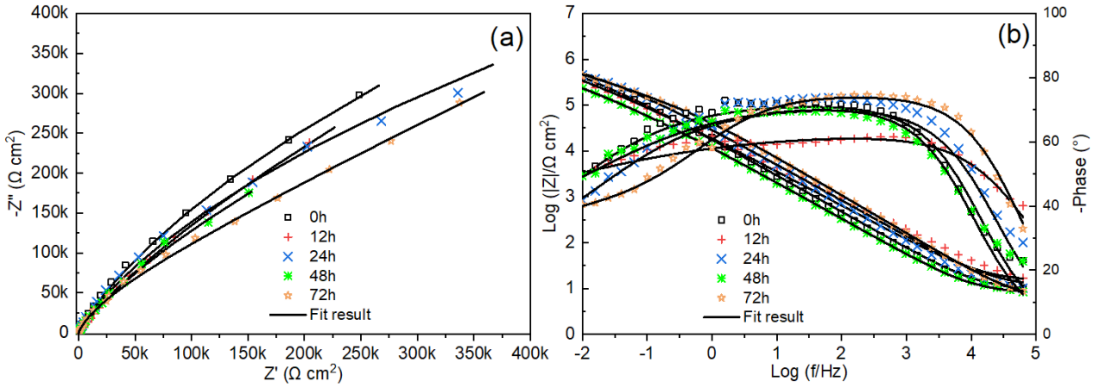

Figure 9. (a) Nyquist plots and (b) Bode Plots of the slippery surfaces after immersion into 3.5 wt.% NaCl solution for various time.

EIS measurements were also carried out to quantify the corrosion resistant stability of the slippery surface in NaCl solution under different immersion time. It can be observed from Nyquist plots shown in Fig. 9a that all the curves appear to be similar in terms of their shape and size, inferring that the diameters of capacitive loops did not change much within 72 hours immersion. Then the Nyquist plots were fitted using the equivalent circuit model inserted in Fig. 5b, and the extracted parameters are displayed in Table S3 (Supporting Information). Even after 72 hours, the fitted charge transfer resistance (R_{ct}) of immersed slippery surface was reduced to 7689 kΩ cm^2, but still much greater than the fresh super-hydrophobic surface (95.32 kΩ cm^2) and the pristine steel substrate (1.58 kΩ cm^2). In addition, it is obviously noted from Fig. 9b that the immersed slippery surface retained a high impedance value in low frequency at approximately $10^{5.5}$ Ω cm^2 within 72 hours immersion into 3.5 wt.% NaCl solution, almost keeping one order of magnitude higher than the fresh super-hydrophobic surface and two order of magnitude greater than the pristine steel substrate. It is therefore

concluded that the oil-infused slippery surface could exhibit much more stable anticorrosive performance than the super-hydrophobic surface and other reference samples. The as-prepared slippery surface can offer effective protection for the base substrate due to the excellent insulation between the corrosive medium and the metal surface.

4. Conclusions

To conclude, a super-hydrophobic coating on stainless steel was fabricated by nanosecond laser ablation combining fluoroalkylsilane modification. Slippery coating was obtained by further infusion of lubricating oil into the as-prepared super-hydrophobic substrate. The formation mechanism of the super-hydrophobicity was proposed. The electrochemical measurements demonstrate that both the super-hydrophobic and slippery coating presented excellent corrosion protection for the base steel material. However, the super-hydrophobic surface would quickly lose its super-hydrophobicity after immersed into 3.5 wt.% NaCl solution for 24 hours, showing a relatively poor stability due to the destroy of unstable air layer. As a result, the contact area between the corrosive ions and the substrate will be enlarged, leading to the severe degradation of base material. In contrast, the slippery coating showed exceptional anticorrosive performance posterior to long-term immersion to corrosive solution. The results indicate that the oil-impregnated slippery coating exhibited superior corrosion prevention than the super-hydrophobic coating. Therefore, the authors believe this study is expected to promote the development of anticorrosive coating for stainless steel materials.

Acknowledgements

This work received financial supports from Program of International S&T Cooperation (2016YFE0112100), National Key R&D Program of China (No. 2017YFB1104700), Science & Technology Commission of Tianjin Municipality (18PTZWHZ00160), H2020 Project (MNR4SCell 734174), and National Natural Science Foundations of China (Nos. 51675371, 51675376 and 51675367). The authors would like to thank Professor Zuobin Wang and Zhankun Weng from CUST for technical supports.

References:

[1] X. Li, D. Zhang, Z. Liu, Z. Li, C. Du, C. Dong, Materials science: share corrosion data, Nature 527 (2015) 441-442.

[2] T. Xiang, Y. Han, Z. Guo, R. Wang, S. Zheng, S. Li, C. Li, X. Dai, Fabrication of inherent anticorrosion superhydrophobic surfaces on metals, ACS Sustainable Chem. Eng. 6 (2018) 5598-5606.

[3] T.M. Yue, J.K. Yu, H.C. Man, The effect of excimer laser surface treatment on pitting corrosion resistance of 316LS stainless steel, Surf. Coat. Technol. 137 (2001) 65-71.

[4] T. Xiang, S. Ding, C. Li, S. Zheng, W. Hu, J. Wang, P. Liu, Effect of current density on wettability and corrosion resistance of superhydrophobic nickel coating deposited on low carbon steel, Mater. Des. 114 (2017) 65-72.

[5] E. Alibakhshi, M. Akbarian, M. Ramezanzadeh, B. Ramezanzadeh, M. Mahdavian, Evaluation of the corrosion protection performance of mild steel coated with hybrid sol-gel silane coating in 3.5 wt.% NaCl solution, Prog. Org. Coat. 123 (2018) 190-200.

[6] Z.B. Wang, Z.Y. Wang, H.X. Hu, C.B. Liu, Y.G. Zheng, Corrosion protection performance of nano-SiO_2/epoxy composite coatings in acidic desulfurized flue gas condensates, J. Mater. Eng. Perform. 25 (2016) 3880-3889.

[7] J. Mondal, A. Marques, L. Aarik, J. Kozlova, A. Simões, V. Sammelselg, Development of a thin ceramic-graphene nanolaminate coating for corrosion protection of stainless steel. Corros. Sci. 105 (2016) 161-169.

[8] J.T. Tian, X.Z. Liu, J.F. Wang, X. Wang, Y.S. Yin, Electrochemical anticorrosion behaviors of the electroless deposited Ni-P and Ni-P-PTFE coatings in sterilized and unsterilized seawater, Mater. Chem. Phys. 124 (2010) 751-759.

[9] D.Y. Yu, J.F. Wang, J.T. Tian, X.M. Xu, J.H. Dai, X. Wang, Preparation and characterization of TiO_2/ZnO composite coating on carbon steel surface and its anticorrosive behavior in seawater, Composites, Part B 46 (2013) 135-144.

[10] Z. Shi, Y. Ouyang, R. Qiu, S. Hu, Y. Zhang, M. Chen, P. Wang, Bioinspired superhydrophobic and oil-infused nanostructured surface for Cu corrosion

inhibition: a comparison study, Prog. Org. Coat. 131 (2019) 49-59.

[11] A.J. Jadhav, C.R. Holkar, D.V. Pinjari, Anticorrosive performance of super-hydrophobic imidazole encapsulated hollow zinc phosphate nanoparticles on mild steel, Prog. Org. Coat. 114 (2018) 33-39.

[12] Z. Lian, J. Xu, Z. Yu, P. Yu, H. Yu, A simple two-step approach for the fabrication of bio-inspired superhydrophobic and anisotropic wetting surfaces having corrosion resistance, J. Alloys Compd. 793 (2019) 326-335.

[13] U. Trdan, M. Hočevar, P. Gregorčič, Transition from superhydrophilic to superhydrophobic state of laser textured stainless steel surface and its effect on corrosion resistance, Corros. Sci. 123 (2017) 21-26.

[14] S.F. Toosi, S. Moradi, M. Ebrahimi, S.G. Hatzikiriakos, Microfabrication of polymeric surfaces with extreme wettability using hot embossing, Appl. Surf. Sci. 378 (2016) 426-434.

[15] C.H. Xue, Y.R. Li, P. Zhang, J.Z. Ma, S.T. Jia, Washable and wear-resistant superhydrophobic surfaces with self-cleaning property by chemical etching of fibers and hydrophobization, ACS Appl. Mater. Interfaces 6 (2014) 10153-10161.

[16] S.A. Kamal, R. Ritikos, S.A. Rahman, Wetting behavior of carbon nitride nanostructures grown by plasma enhanced chemical vapor deposition technique, Appl. Surf. Sci. 328 (2015) 146-153.

[17] Y. Huang, D.K. Sarkar, D. Gallant, X.G. Chen, Corrosion resistance properties of superhydrophobic copper surfaces fabricated by one-step electrochemical modification process, Appl. Surf. Sci. 282 (2013) 689-694.

[18] R.V. Lakshmi, B.J. Basu, Fabrication of superhydrophobic sol-gel composite films using hydrophobically modified colloidal zinc hydroxide, J. Colloid. Interface Sci. 339 (2009) 454-460.

[19] Y. Tuo, W. Chen, H. Zhang, P. Li, X. Liu, One-step hydrothermal method to fabricate drag reduction superhydrophobic surface on aluminum foil, Appl. Surf. Sci. 446 (2018) 230-235.

[20] Y. Liu, S.Y. Li, J.J. Zhang, J.A. Liu, Z.W. Han, L.Q. Ren, Corrosion inhibition of biomimetic super-hydrophobic electrodeposition coatings on copper substrate,

581 Corros. Sci. 94 (2015) 190-196.
582 [21] B.X. Zheng, G.D. Jiang, W.J. Wang, X.S. Mei, Fabrication of superhydrophilic or
583 superhydrophobic self-cleaning metal surfaces using picosecond laser pulses and
584 chemical fluorination, Radiat. Eff. Defects Solids 171 (2016) 461-473.
585 [22] A.F. Pan, W.J. Wang, X.S. Mei, K.D. Wang, X.B. Yang, Rutile TiO_2 flocculent
586 ripples with high antireflectivity and superhydrophobicity on the surface of
587 titanium under 10 ns laser irradiation without focusing, Langmuir 33 (2017) 9530-
588 9538.
589 [23] C.J. Yang, Y.C. Zhao, Y.L. Tian, F.J. Wang, X.P. Liu, X.B. Jing, Fabrication and
590 stability investigation of bio-inspired superhydrophobic surface on nitinol alloy,
591 Colloids Surf., A 567 (2019) 16-26.
592 [24] Z. Xia, Y. Xiao, Z. Yang, L. Li, S. Wang, X. Liu, Y. Tian, Droplet impact on the
593 super-hydrophobic surface with micro-pillar arrays fabricated by hybrid laser
594 ablation and silanization process, Materials, 12 (2019) 765.
595 [25] J. Fahim, S.M.M. Hadavi, H. Ghayour, S.A.H. Tabrizi, Cavitation erosion
596 behavior of super-hydrophobic coatings on Al5083 marine aluminum alloy, Wear,
597 424-425 (2019) 122-132.
598 [26] R. Poetes, K. Holtzmann, K. Franze, U. Steiner, Metastable underwater
599 superhydrophobicity, Phys. Rev. Lett. 105 (2010) 166104.
600 [27] T.S. Wong, S.H. Kang, S.K. Tang, E.J. Smythe, B.D. Hatton, A. Grinthal, J.
601 Aizenberg, Bioinspired self-repairing slippery surfaces with pressure-stable
602 omniphobicity, Nature 477 (2011) 443-447.
603 [28] J. Zhang, C. Gu, W. Yan, J. Tu, X. Ding, Fabrication and corrosion property of
604 conversion films on magnesium alloy from deep eutectic solvent, Surf. Coat.
605 Technol. 344 (2018) 702-709.
606 [29] Z. Shi, Y. Xiao, R. Qiu, S. Niu, P. Wang, A facile and mild route for fabricating
607 slippery liquid-infused porous surface (SLIPS) on CuZn with corrosion resistance
608 and self-healing properties, Surf. Coat. Technol. 330 (2017) 102-112.
609 [30] Y. Xu, M. Liu, Soiling and corrosion behaviors on fluorinated anodized TiO_2
610 surface infused by perfluoropolyether, Surf. Coat. Technol. 307 (2016) 332-344.

611 [31] J. Yong, F. Chen, Q. Yang, J. Huo, X. Hou, Superoleophobic surfaces, Chem. Soc.
612 Rev. 46 (2017) 4168-4217.
613 [32] J. Li, E. Ueda, D. Paulssen, P. Levkin, Slippery lubricant-infused surfaces:
614 properties and emerging applications, Adv. Funct. Mater. 29 (2019) 1802317.
615 [33] J. Zhang, Z. Yao, Slippery properties and the robustness of lubricant-impregnated
616 surfaces, J. Bionic Eng. 26 (2019) 291-298.
617 [34] Z. Yang, Y. Tian, C. Yang, F. Wang, X. Liu, Modification of wetting property of
618 Inconel 718 surface by nanosecond laser texturing, Appl. Surf. Sci. 414 (2017)
619 313-324.
620 [35] Z. Yang, X. Liu, Y. Tian, Insights into the wettability transition of nanosecond
621 laser ablated surface under ambient air exposure, J. Colloid. Interface Sci. 533
622 (2019) 268-277.
623 [36] Y. Tian, Y. Zhao, C. Yang, F. Wang, X. Liu, X. Jing, Fabrication of bio-inspired
624 nitinol alloy surface with tunable anisotropic wetting and high adhesive ability, J.
625 Colloid. Interface Sci. 527 (2018) 328-338.
626 [37] Z. Yang, Y. Tian, Y. Zhao, C. Yang, Study on the fabrication of super-
627 hydrophobic surface on Inconel alloy via nanosecond laser ablation, Materials, 12
628 (2019) 278.
629 [38] F. Song, C. Wu, H. Chen, Q. Liu, J. Liu, R. Chen, R. Li, J. Wang, Water-repellent
630 and corrosion-resistance properties of superhydrophobic and lubricant-infused
631 super slippery surfaces, RSC Adv. 7 (2017) 44239-44246.
632 [39] S. Yuan, S.O. Pehkonen, B. Liang, Y.P. Ting, K.G. Neoh, E.T. Kang,
633 Superhydrophobic fluoropolymer-modified copper surface via surface graft
634 polymerisation for corrosion protection, Corros. Sci. 53 (2011) 2738-2747.
635 [40] Z. Yang, X. Liu, Y. Tian, Hybrid laser ablation and chemical modification for fast
636 fabrication of bio-inspired super-hydrophobic surface with excellent self-cleaning,
637 stability and corrosion resistance, J. Bionic. Eng. 16 (2019) 13-26.
638 [41] J. Yong, J. Huo, Q. Yang, F. Chen, Y. Fang, X. Wu, L. Liu, X. Lu, J. Zhang, X.
639 Hou, Femtosecond Laser Direct Writing of Porous Network Microstructures for
640 Fabricating Super-Slippery Surfaces with Excellent Liquid Repellence and Anti-

641 Cell Proliferation, Adv. Mater. Interfaces 5 (2018) 1701479.
642 [42] Z. Qiu, R. Qiu, Y. Xiao, J. Zheng, C. Lin, Slippery liquid-infused porous surface
643 fabricated on CuZn: A barrier to abiotic seawater corrosion and microbiologically
644 induced corrosion, Appl. Surf. Sci. 457 (2018) 468-476.
645 [43] Q. Ma, W. Wang, G. Dong, Facile fabrication of biomimetic liquid-infused
646 slippery surface on carbon steel and its self-cleaning, anti-corrosion, anti-frosting
647 and tribological properties, Colloids Surf., A 577 (2019) 17-26.
648 [44] Z.G. Qi Li, Lubricant-infused slippery surfaces: facile fabrication, unique liquid
649 repellence and antireflective properties, J. Colloid Interface Sci. 536 (2019) 507-
650 515.
651 [45] Z.M. Shi, M. Liu, A. Atrens, Measurement of the corrosion rate of magnesium
652 alloys using Tafel extrapolation, Corros. Sci. 52 (2010) 579-588.
653 [46] K.M. ŁeRcka, A.J. Antończak, B. Szubzda, M.R. Wójcik, B.D. Stępak, P.
654 Szymczyk, M. Trzciński, M. Ozimek, K.M. Abramski, Effects of laser-induced
655 oxidation on the corrosion resistance of AISI 304 stainless steel, J. Laser Appl. 28
656 (2016) 032009.
657 [47] Y. Liu, X. Yin, J, Zhang, S. Yu, Z. Wu, L. Ren, A electro-deposition process for
658 fabrication of biomimeticsuper-hydrophobic surface and its corrosion resistance
659 on magnesium alloy, Electrichim. Acta, 125 (2014) 395-403.
660 [48] W. Liu, Q. Xu, J. Han, X. Chen, Y. Min, A novel combination approach for the
661 preparation of superhydrophobic surface on copper and the consequent corrosion
662 resistance, Corros. Sci. 110 (2016) 105-113.
663 [49] B. Hirschorn, M.E. Orazem, B. Tribollet, V. Vivier, I. Frateur, M. Musiani,
664 Determination of effective capacitance and film thickness from constant-phase-
665 element parameters, Electrochim. Acta 55 (2010) 6218-6227.
666 [50] D. Li, H. Wang, Y. Liu, D. Wei, Z. Zhao, Large-scale fabrication of durable and
667 robust super-hydrophobic spray coatings with excellent repairable and anti-
668 corrosion performance, Chem. Eng. J. 367 (2019) 169-179.
669 [51] T. Ishizaki, Y. Masuda, M. Sakamoto, Corrosion resistance and durability of
670 superhydrophobic surface formed on magnesium alloy coated with nanostructured

671 cerium oxide film and fluoroalkylsilane molecules in corrosive NaCl aqueous
672 solution, Langmuir 27 (2011) 4780-4788.
673 [52] T. Xiang, M. Zhang, H.R. Sadig, Z. Li, M. Zhang, C. Dong, L. Yong, W. Chan,
674 C. Li, Slippery liquid-infused porous surface for corrosion protection with self-
675 healing property, Chem. Eng. J. 345 (2018) 147-155.

Supporting Information

A contrastive investigation on anticorrosive performance of laser-induced super-hydrophobic and oil-infused slippery coatings

Zhen Yang, Xianping Liu, Yanling Tian*

School of Engineering, University of Warwick, Coventry CV4 7AL, UK

Corresponding author:

E-mail address: meytian@tju.edu.cn, Y.Tian.1@warwick.ac.uk

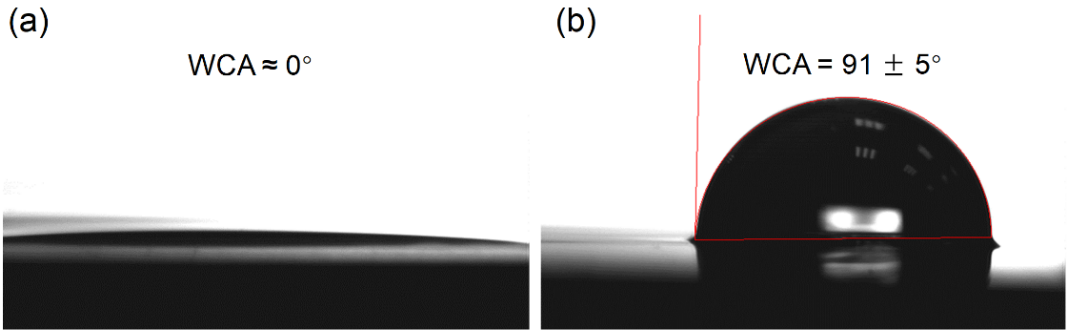

Figure S1. WCA values of (a) initial laser-processing surface, (b) pristine 316L substrate with silicon oil coating.

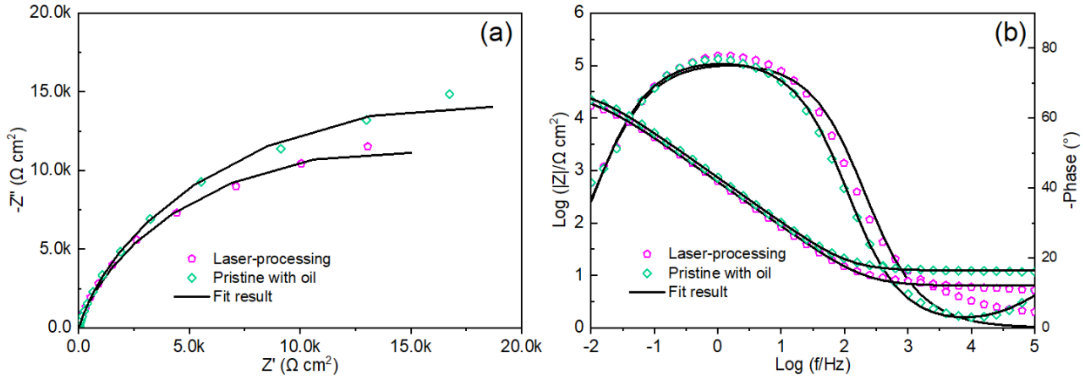

Figure S2. (a) Nyquist plots and (b) Bode Plots of the initial laser-processing surface and pristine 316L substrate with silicon oil coating. The fit result was received based on the equivalent circuit displayed in Fig. 5b.

Table S1. The fitting parameters of the elements in the equivalent circuit models.

Sample	R_s	R_{ct}	CPE_{dl}		R_f	CPE_f	
	Ω cm²	kΩ cm²	Q_{dl}	α_{dl}	kΩ cm²	Q_f	α_f
Pristine	5.32	1.58	26.0	0.79	-	-	-
Laser-processing	6.34	23.56	34.3	0.85	6.51	48.8	0.80
Pristine with oil	7.68	33.51	85.3	0.81	6.65	27.8	0.86
Super-hydrophobic	6.33	95.32	7.41	0.80	7.98	1.49	0.76

Slippery	9.03	10300	0.31	0.32	2144	1.21	0.80

Table S2. The evolution of WCA and SA for the as-prepared super-hydrophobic and slippery surfaces with different immersion time in 3.5 wt.% NaCl solution.

Sample	Super-hydrophobic		Slippery	
	WCA	SA	WCA	SA
Slippery (0 hour)	158 ± 2º	2 ± 1º	106 ± 2º	5 ± 2º
After 12 hours	151 ± 3º	7 ± 3º	105 ± 2º	7 ± 3º
After 24 hours	145 ± 6º	30 ± 6º	104 ± 2º	9 ± 3º
After 48 hours	125 ± 8º	65 ± 10º	103.5± 2.5º	10 ± 4º
After 72 hours	112 ± 10º	90º	103 ± 3º	12 ± 5º

Table S3. The fitting parameters extracted from Nyquist plots in Fig. 9a.

Sample	R_s	R_{ct}	CPE_{dl}		R_f	CPE_f	
	Ω cm^2	kΩ cm^2	Q_{dl}	α_{dl}	kΩ cm^2	Q_f	α_f
Slippery (0 hour)	9.03	10300	0.31	0.32	2144	1.21	0.80
After 12 hours	13.98	11600	0.46	0.38	2610	1.35	0.76
After 24 hours	11.28	9210	0.29	0.31	1869	0.73	0.79
After 48 hours	7.85	8326	0.76	0.39	1356	1.70	0.80
After 72 hours	5.82	7689	0.63	0.42	1128	0.44	0.83